Supplementary information

Table S1 Comparison of various titanium oxide anode systems.

	Reversible Capacity/ $mAhg^{-1}$	Average Voltage/V	Energy Density(Wh/kg)		
			4V cathode	3.5V cathode	3.3V cathode
O3-$NaTiO_2$	152	1.0	**456**	**380**	**350**
P2-$Na_{0.66}[Li_{0.22}Ti_{0.78}]O_2$	110	0.75	**357**	**302**	**280**
$Li_4Ti_5O_{12}$	155	0.91	479	401	370

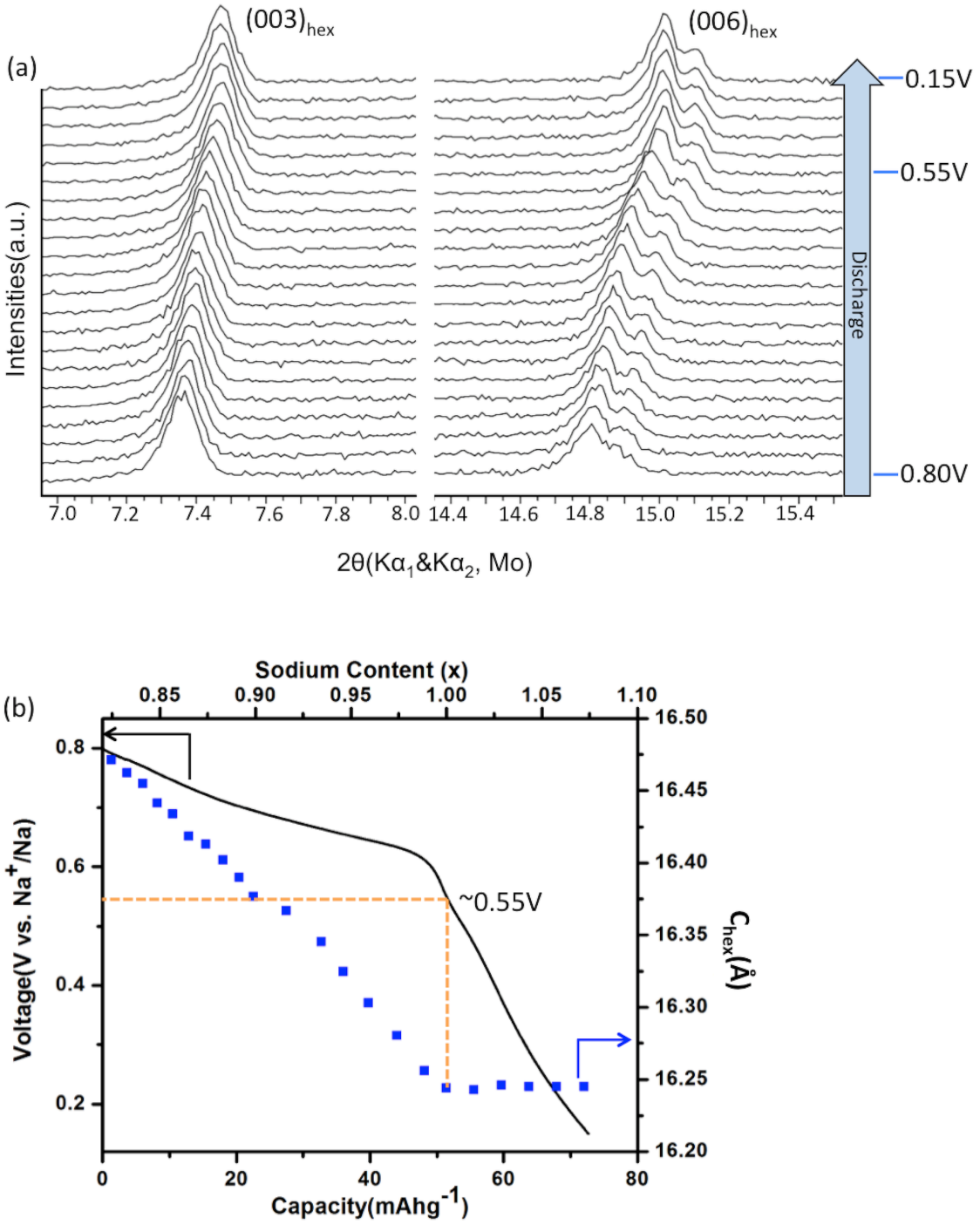

Figure S1. Structural evolution during electrochemical sodiation of O3-$NaTiO_2$. (a) *In situ* XRD data recorded during the first galvanostatic discharge at a current rate of C/20 in the voltage range between 0.8 V and 0.15 V. The main peaks are centered around the $(003)_{hex}$ and $(006)_{hex}$ reflections. (b) Evolution of cell voltage and interslab distance as a function of sodium content.

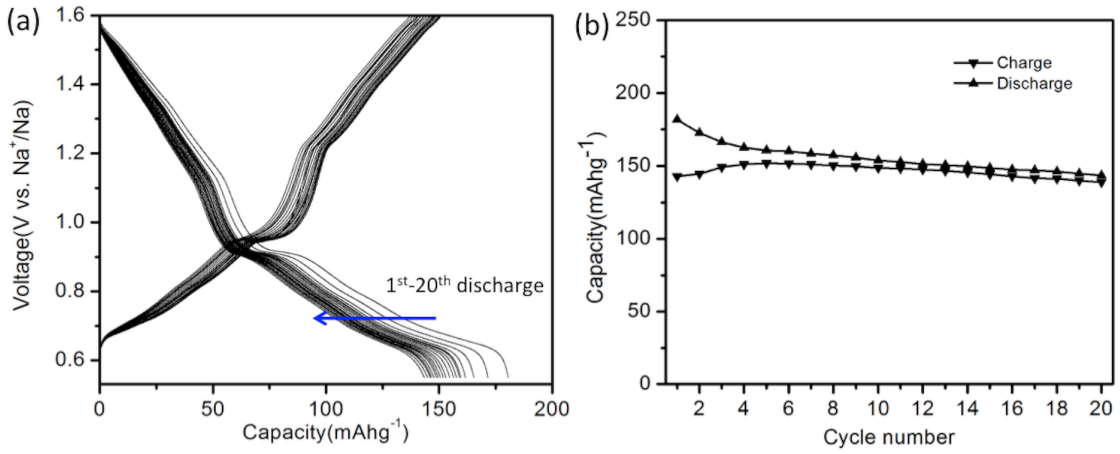

Figure S2. (a) Galvanostatic charge/discharge curves at a current rate of C/10 in the voltage range of 0.55 V-1.6 V. (b) Cycling performance. The charge/discharge capacity versus cycle number of the corresponding galvanostatic battery test.

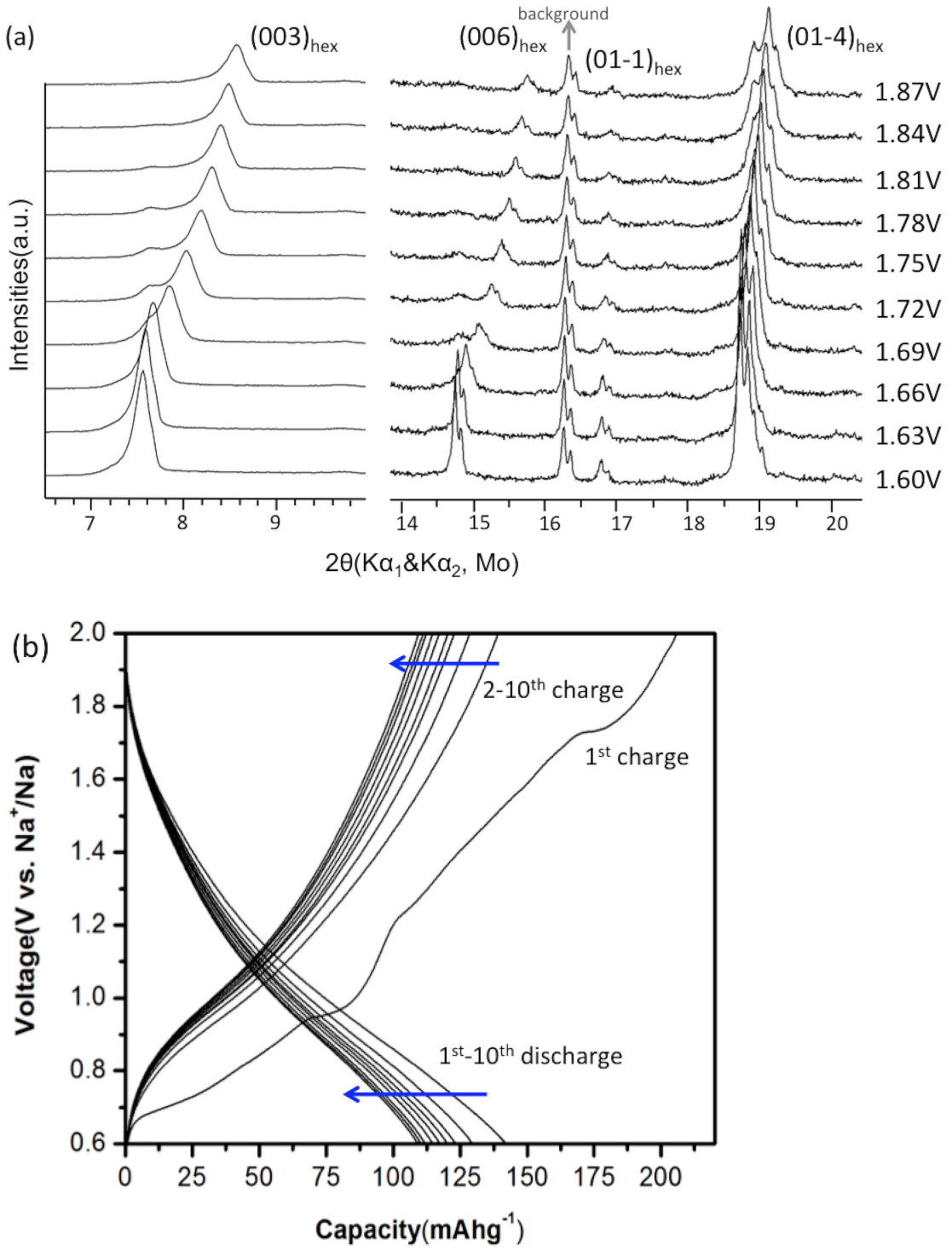

Figure S3. (a) Structural evolution during electrochemical desodiation of $NaTiO_2$. *In situ* XRD data recorded during the PITT charge in the voltage range between 1.6 V and 1.87 V. The main peaks correspond to $(003)_{hex}$, $(006)_{hex}$, $(01\text{-}1)_{hex}$ and $(01\text{-}4)_{hex}$ reflections, respectively. (b) Galvanostatic charge/discharge curves at a current rate of C/10 in the voltage range of 0.6 V-2.0 V.

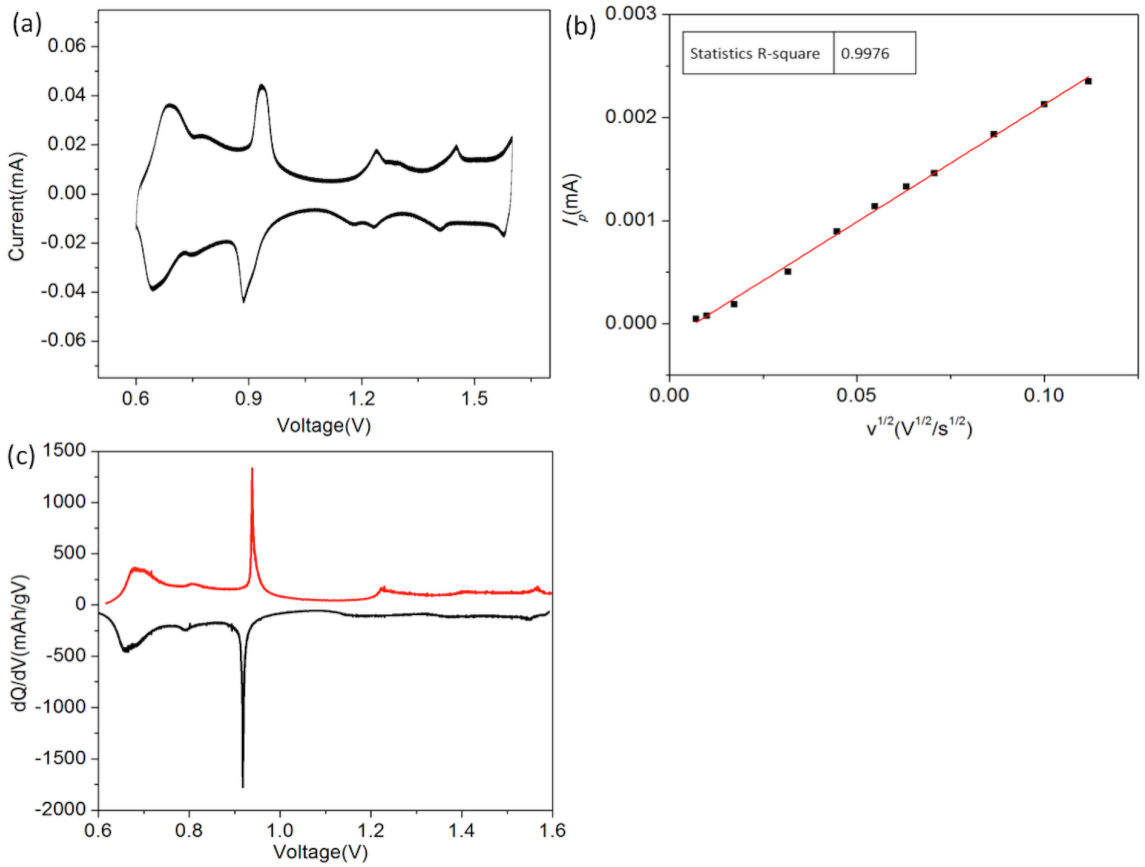

Figure S4. (a) Cyclic voltammogram of $NaTiO_2$ at 0.05mV/s sweep rate in the voltage range of 0.6-1.6 V. (b) Relationship between peak current *Ip* and square root of scan rate $v^{1/2}$. (c) First differential curve of specific capacity over voltage.

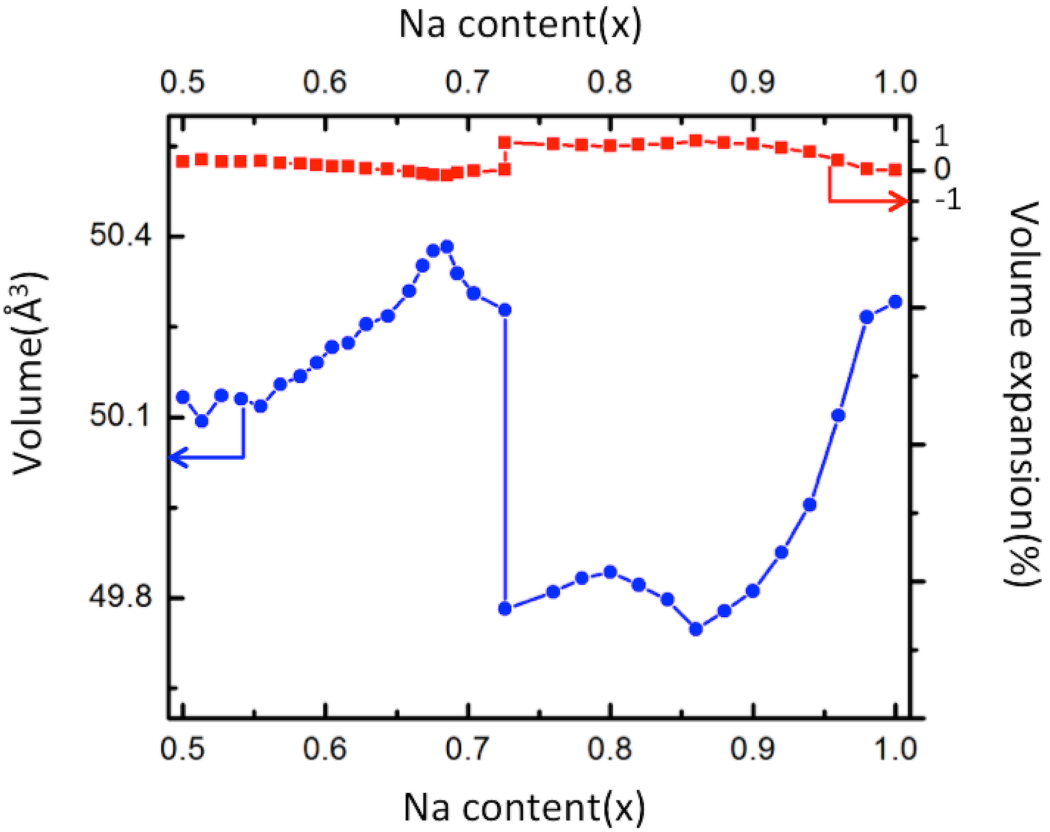

Figure S5. Volume of Na_xTiO_2 primitive cell as a function of sodium content and corresponding expansion percentage relative to Na_1TiO_2.